PABP Interacting Protein 2A (PAIP2A) Regulates Specific Key Proteins During Spermiogenesis in the Mouse 1

Authors: Delbes, Geraldine, Yanagiya, Akiko, Sonenberg, Nahum, and Robaire, Bernard

Source: Biology of Reproduction, 86(3) : 95

Published By: Society for the Study of Reproduction

URL: https://doi.org/10.1095/biolreprod.111.092619

BIOLOGY OF REPRODUCTION (2012) **86**(3):95, 1–8
Published online before print 21 December 2011.
DOI 10.1095/biolreprod.111.092619

PABP Interacting Protein 2A (PAIP2A) Regulates Specific Key Proteins During Spermiogenesis in the Mouse[1]

Geraldine Delbes,[3,4] Akiko Yanagiya,[3,5,6] Nahum Sonenberg,[5,6] and Bernard Robaire[2,4,7]

[4]*Department of Pharmacology and Therapeutics, McGill University, Montreal, Quebec, Canada*
[5]*Department of Biochemistry, McGill University, Montreal, Quebec, Canada*
[6]*The Goodman Cancer Research Centre, McGill University, Montreal, Quebec, Canada*
[7]*Department of Obstetrics and Gynecology, McGill University, Montreal, Quebec, Canada*

ABSTRACT

During spermiogenesis, expression of the specific proteins needed for proper differentiation of male germ cells is under translational control. We have shown that PAIP2A is a major translational regulator involved in the maturation of male germ cells and male fertility. To identify the proteins controlled by PAIP2A during spermiogenesis, we characterized the proteomic profiles of elongated spermatids from wild-type (WT) mice and mice that were *Paip2a/Paip2b* double-null mutants (DKO). Elongated spermatid populations were obtained and proteins were extracted and separated on gradient polyacrylamide gels. The gels were digested with trypsin and peptides were identified by mass spectrometry. We identified 632 proteins with at least two unique peptides and a confidence level of 95%. Only 209 proteins were consistently detected in WT or DKO replicates with more than five spectra. Twenty-nine proteins were differentially expressed with at least a 1.5-fold change; 10 and 19 proteins were down- and up-regulated, respectively, in DKO compared to WT mice. We confirmed the significantly different expression levels of three proteins, EIF4G1, AKAP4, and HK1, by Western blot analysis. We have characterized novel proteins that have their expression controlled by PAIP2A; of these, 50% are involved in flagellar structure and sperm motility. Although several proteins affected by abrogation of *Paip2a* have established roles in reproduction, the roles of many others remain to be determined.

elongated spermatids, gene expression, PAIP2A, proteomics, spemiogenesis, tail structure, translational control

INTRODUCTION

Spermatogenesis is the process by which male germ cells become highly differentiated haploid spermatozoa. This complex process requires expression of specific proteins at very specific steps of cell differentiation, and so displays tightly controlled transcriptional and translational regulations. Some major factors of transcriptional regulation in spermatogenesis have been identified as DNA binding proteins, transcription factors, and chromatin remodeling factors (see review in [1]), but translational control during spermatogenesis remains largely elusive. RNA-binding proteins and the shortening of the mRNA poly (A) tail are believed to be involved in this process [2–9]. RNA binding proteins such as SAM68 (official symbol KHDRBS1) [10], GRTH (official symbol DDX25) [11], and YBX2 (also known as MSY2) [7] have been shown to be essential for translational control during spermatogenesis. Mice carrying a null mutation for *Sam68* show an early arrest in spermatogenesis around the pachytene spermatocyte stage, whereas knockouts for *Grth* and *Ybx2* result in spermatogenic arrest in late round spermatids, suggesting that these proteins play different roles at different steps of spermatogenesis.

Other factors, such as PTBP2 and PABP, play important roles in RNA storage and stabilization of mRNA during spermatogenesis [2, 5]. We have recently shown that a PABP partner, PAIP2A, is also an essential player in translational control during late spermiogenesis [12]. PAIP2A has been described as a translational inhibitor in vitro; it competes with EIF4G for PABP binding and decreases the PABP affinity for the mRNA poly (A) tails [13, 14]. There are two isoforms of PAIP2: PAIP2A and PAIP2B. PAIP2A is highly expressed in the testis and pancreas, while PAIP2B is highly expressed in the pancreas. PAIP2A is specifically expressed in the cytoplasm of late spermatids during spermiogenesis [12]. We have previously shown by immunohistochemistry [12] that PAIP2A expression becomes increased in late elongated spermatids as PABP expression becomes decreased, while PAIP2B is barely expressed in these cells.

The regulation of poly (A) tail length by polyadenylation or deadenylation is one of the key mechanisms of gene expression in spermatogenesis. For example, PAPOLB (also known as TPAP) is involved in poly (A) tail extension in round spermatids, and *Papolb*-KO mice exhibit spermatogenetic arrest [15]. Kleene and colleagues [4, 16] have shown that during spermiogenesis, the shortening of the poly (A) tail in elongated spermatids is correlated with active translation, suggesting an important role for PABP. We have demonstrated that efficient mRNA translation in late spermiogenesis occurs at an optimal concentration of PABP, and that it is regulated by PAIP2A [12].

Male *Paip2a*/*Paip2b*-DKO mice, as well as *Paip2a*-KO mice, are infertile due to specific defects in spermiation and the differentiation of elongated spermatids [12]. In the *Paip2a*-KO and *Paip2a*/*Paip2b*-DKO, elongated spermatids at Stage 7 of spermatogenesis show multiple structural abnormalities, including impairment of flagellum formation, absence of the mitochondrial sheath in the middle piece, as well as abnormal chromatin condensation and acrosomal development [12]. The

[1]Supported by grants from the Canadian Institutes of Health Research.
[2]Correspondence: Bernard Robaire, Department of Pharmacology and Therapeutics, McGill University, 3655 Promenade Sir-William Osler, Montréal, Québec, Canada H3G 1Y6.
E-mail: bernard.robaire@mcgill.ca
[3]These authors contributed equally to this work.

Received: 30 March 2011.
First decision: 27 April 2011.
Accepted: 23 November 2011.

eISSN: 1529-7268 http://www.biolreprod.org
ISSN: 0006-3363

large numbers of defects observed in the *Paip2a*/*Paip2b*-DKO elongated spermatids strongly suggest that key proteins needed for proper cell differentiation are not generated in the absence of PAIPA2.

We hypothesized that PAIPA2 plays an important role in late spermiogenesis by regulating the expression of key proteins for male germ cell differentiation. To investigate which proteins are regulated by PAIP2A during spermiogenesis, a wide-ranging proteomic analysis was undertaken. We have identified a group of proteins that is differentially expressed in elongated spermatids between WT and *Paip2a*/*Paip2*b-DKO mice.

MATERIALS AND METHODS

Animals

Male *Paip2a*/*Paip2b*-DKO mice [12] were housed on a 12L:12D cycle with food and water provided ad libitum. All animal studies were conducted in accordance with the guidelines outlined in *A Guide to the Care and Use of Experimental Animals*, prepared by the Canadian Council on Animal Care (McGill Animal Resources Centre protocol 5505). Mice (10 to 12 weeks old) were euthanized by CO_2 asphyxiation; their testes were removed, decapsulated, and flash frozen in liquid nitrogen for whole testis extract or used for further isolation of spermatogenic cells by unit gravity cell separation.

Cell Separation

Spermatogenic cells were obtained through cell separation by velocity sedimentation using the STA-PUT method as previously described by Bellvé et al. [17]. Briefly, the testes of five mice were decapsulated and digested by enzymatic treatment at 34°C with 0.5 mg/ml collagenase (C9891; Sigma, Oakville, ON, Canada) for 12 min, followed by 0.5 mg/ml trypsin (T8003; Sigma) for 16 min. Cells were then suspended by gentle pipetting in the presence of 1 μg/ml DNase I (DN-25; Sigma), and filtered through a nylon mesh and washed with RPMI medium containing 0.5% BSA fraction V. Of these, 3×10^8 cells were loaded in the velocity sedimentation apparatus (STA-PUT; Proscience, Don Mills, ON, Canada), followed by 2%–4% BSA gradient in RPMI. Fractions containing pachytene spermatocytes, round spermatids from spermiogenesis Stages 1 to 8, and a mixture of elongating and elongated spermatids from spermiogenesis Stages 8 to 16 were identified by phase-contrast microscopy using cell morphology criteria as previously described (Supplemental Fig. S1; all Supplemental Data are available online at www.biolreprod.org) [18]. Fractions with higher than 85% purity were pooled and stored at −80°C for RNA and protein extraction.

As assessed by counting nucleated cells, elongated spermatids constituted 94.1 ± 1.5% and 93.7 ± 1.3% of the cells in the elongated spermatid fraction in the WT and the *Paip2a*/*Paip2b*-DKO mice, respectively. Despite the defects in spermiogenesis in *Paip2a*/*Paip2b*-DKO mice, no apparent difference could be observed in the different fractions obtained when compared to WT (Supplemental Fig. S1). It is important to note that using the STA-PUT method, the elongated spermatid fraction contains a mixture of nuclear and anucelate cytoplasmic fragments of elongated spermatids, residual bodies, and anucleate cytoplasmic fragments of other cell types that cannot be identified by phase contrast microscopy [22]. We calculated that the residual bodies represented about 70% of the sample (72 ± 7% in WT mice [n = 6], and 73 ± 8% in *Paip2a*/*Paip2b*-DKO mice [n = 4]). Therefore, we were analyzing the proteins from each cellular compartment of the spermatids, including the cytoplasm that is shed in later spermiation.

Proteomics

Pellets obtained from 2×10^6 elongated spermatids (n = 3, WT and *Paip2a*/*Paip2b*-DKO) were thawed on ice and placed in 175 μl of Laemmli buffer (2% SDS, 10% glycerol, 5% 2-mercaptoethanol, 0.002% bromphenol blue, and 62.5 mM Tris-HCl). The samples were homogenized with an ultrasonicator (Sonics & Materials, Inc., Newtown, CT) and centrifuged at 10 000 × *g* for 10 min at 4°C. The remaining supernatant from each sample was aliquoted and stored at −20°C for protein assay using the 2D Quant Protein Assay (GE Healthcare, Baie d'Urfe, QC, Canada). In collaboration with Genome Quebec, proteins from each sample (30 μg) were separated on a 2.4-cm, 7%-to-15% SDS-acrylamide gel electrophoresis (Supplemental Fig. S2). Each lane was then robotically excised with the Pro-XCISION Proteomics Gel Cutting Robot (PerkinElmer) in 15 bands that were further subjected to in-gel digestion for 4.5 h with 6 ng/μl of trypsin (Promega Gold) in 100 mM ammonium bicarbonate. Sample injection and HPLC separation was done using an Agilent 1100 series system. Mass spectrometric analysis was conducted using the Micro-Qtof from Waters (Milford, MA). The scan range was 350 m/z to 1600, which means a minimum size of 750 Da for a doubly charged peptide (on average, six amino acids) to an upper limit of 4800 Da for a triply charged peptide. Some small-sized peptides may also have been too hydrophilic to be retained by the c18 column. Peptides and proteins were first identified using Mascot 2.1 (www.matrixscience.com) against a uniprot_database from November 2008 filtered for *Mus musculus* proteins (60 636 entries) using trypsin as digestion enzyme with one miscleavage allowed, carboxyamidomethylation of cysteines as fixed modification, methionine oxydation as variable modification, and 0.5 Da precursor and 0.5 fragment search tolerances. An additional search using X! Tandem (http://www.thegpm.org/TANDEM/) was carried out on the subset database of identified proteins with additional modifications considered for D/E and c-terminal methylation, proprionamide modification of cysteines, deamidation of N/Q, and pyroglutamic acid formation of n-terminal Q. Results were subsequently analyzed using Scaffold 2.0 (Proteome Software, Inc., Portland, OR). Only peptides for which we had a confidence level of 95% were considered; proteins were identified by at least two unique peptides and a false discovery rate lower than 0.1%. For quantification and further statistical analysis, we used the spectral counting method [19]. Data are expressed as unweighted spectrum count for each protein; this represents the number of times a spectrum was assigned to a peptide belonging to a specific protein.

Real-Time PCR

Total RNA was extracted from the elongated spermatid fractions ($2–6\times10^6$ cells) using TRI-ZOL Reagent (Invitrogen, Burlington, ON, Canada) and reverse-transcribed by SuperScript III RT (Invitrogen) following the manufacturer's instructions. The resultant cDNA was used for real-time PCR using the gene-specific primers for mouse *Eif4g1*, *Wdr62*, *Akap4*, *Hk1*-s (Supplemental Table S1), and β-actin (*Actb*) (mHKG-110; MCLAB, San Francisco, CA). The SYBR Green PCR Master Mix (Applied Biosystems, Carlsbad, CA) was used for real-time PCR using the first-strand cDNA as a template, and real-time PCR was performed in triplicate. The *Actb* mRNA level in each sample was determined to normalize the differences of total RNA amount. Values indicate the relative mRNA levels in *Paip2a*/*Paip2b*-DKO mice as compared with those in WT mice, which were set as one.

Western Blot Analysis

Pachytene spermatocyte, round spermatid, and elongated spermatid pellets ($3–8\times10^6$ cells) were thawed on ice and lysed in RIPA buffer (50 mM Tris-HCl [pH 7.5], 150 mM NaCl, 1% Nonidet P-40, 0.5% deoxycholate, and 0.1% SDS) containing protease inhibitor cocktail (10 μl/ml; P8340; Sigma). Cell lysates were clarified by centrifugation at 13 000 × *g* for 10 min at 4°C. Protein concentrations were measured using the Bio-Rad protein assay (Bio-Rad Laboratories, ON, Canada). Samples (20 μg) were resolved by 8% SDS-PAGE and transferred onto a nitrocellulose membrane (PerkinElmer). Membranes were blocked in 5% nonfat milk in phosphate-buffered saline (PBS) containing 0.1% Tween-20 and probed with primary antibodies against EIF4GI (1:1000 dilution; #2498; Cell Signaling Technologies, Danvers, MA), rabbit anti-mouse AKAP4 (1:5000 dilution) [20], the SSR antiserum (1:1000 dilution) to detect spermatogenic cell-specific type 1 hexokinase [21], and monoclonal anti-β-actin antibody (1:2000 dilution; A5441; Sigma-Aldrich) overnight at 4°C, and subsequently with secondary antibody (ECL anti-rabbit IgG horseradish peroxidase-linked whole antibody; GE Healthcare). Immunoreactive proteins were visualized using enhanced chemiluminescence (Perkin-Elmer). The intensities of the bands were measured using ImageJ software (National Institutes of Health, Bethesda, MD). The value of each band was normalized by that of β-actin.

Statistical Analysis

Experiments were run in triplicate. Two-tailed, unpaired Student *t*-test was used for statistical analysis. The level of significance was taken as $P < 0.05$, unless stated otherwise.

RESULTS

Characterization of Proteins in the Elongated Spermatids

Using 1D gel electrophoresis coupled to mass spectrometry analysis, we were able to characterize the proteins in elongated spermatids and obtained a list of 632 proteins. Of these, 526 proteins were detected in at least one of the three WT

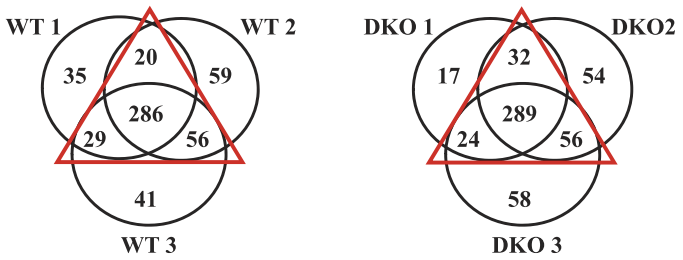

FIG. 1. Numbers of proteins detected in each biological replicate of elongated spermatids. The proteins were extracted from three different cell separations performed on WT (left) or *Paip2a/Paip2b*-DKO (right) mice. Further analysis was performed on the proteins that were detected in at least two replicates (red triangles).

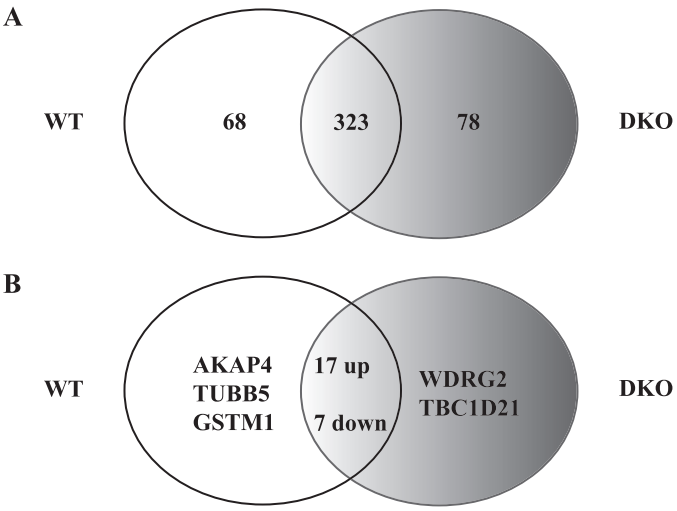

FIG. 2. **A**) Numbers of proteins expressed in the elongated spermatids in WT and *Paip2a/Paip2b*-DKO mice. **B**) Numbers and names of proteins significantly affected in elongated spermatids from *Paip2a/Paip2b*-DKO mice when compared to the WT mice.

replicates, and 530 proteins were detected in one of the three *Paip2a/Paip2b*-DKO replicates (Fig. 1). Interestingly, only 53.7% (286 proteins) and 54.5% (289 proteins) were consistently detected in the three replicates of the WT mice and *Paip2a/Paip2b*-DKO mice, respectively (Fig. 1), suggesting a degree of variability in the detection of peptides by the mass spectrometer. For this reason, in further analysis, we only considered proteins that were detected in at least two replicates of each group; these represent 391 (61.9%) and 401 (63.5%) proteins detected in the WT mice and *Paip2a/Paip2b*-DKO mice, respectively (Fig. 1). In total, 469 proteins were expressed in at least two replicates of one genotype, and 323 were considered expressed in both genotypes (Fig. 2A).

To undertake further quantitative analysis and eliminate false positives, we selected the proteins having average spectrum counts of five or more; these represent 209 proteins (Supplemental Table S2). The most abundant protein found in the WT elongated spermatids was the L-lactate dehydrogenase C chain, representing 3.4% of all spectrum count of the mass spectrometry analysis. It is noteworthy that the basic proteins, known to be essential in chromatin remodeling during spermiogenesis, were not detected in this analysis. Protamines were not detected by the proteomics analysis we used, since they do not resolve in SDS gels; in addition, the peptides generated after trypsin digestion of the transition proteins (i.e., TNP1 and TNP2) were too small to be detected in our analysis. Interestingly, many heat-shock proteins were present in great abundance in the elongated spermatids (i.e., HSP90AA1, HSP90B1, HSPA4L, HSPA8, HSP1L, and HSP90B1), representing a total of 14.4% of the total proteins. Moreover, consistent with our previous result obtained using immunohistochemistry [12], PABP in *Paip2a/Paip2b*-DKO mice was expressed at a higher level than in WT mice (Supplemental Table S2), but the difference was not statistically significant.

Effect of the Lack of PAIP2A and PAIP2B on Protein Expression in Spermiogenesis

In order to identify the proteins whose expression was affected by the lack of PAIP2A and PAIP2B, we undertook a statistical analysis with the proteins having an average spectrum count of five or more (209 proteins; Supplemental Table S2). Interestingly, only 29 (13.8%) of the proteins were significantly affected, with at least a 1.5-fold change in *Paip2a/Paip2b*-DKO mice when compared to WT mice. Two proteins were only detected in *Paip2a/Paip2b*-DKO mice, while three proteins detected in WT mice were never detected in *Paip2a/Paip2b*-DKO mice (Fig. 2B and Table 1). Twenty-four proteins were expressed in both samples, with a significant difference of at least a 1.5-fold change in *Paip2a/Paip2b*-DKO mice as compared with WT mice; seven were down-regulated and 17 were up-regulated in *Paip2a/Paip2b*-DKO mice (Fig. 2B and Table 1). It is interesting to note that 27.6% of these 29 proteins are involved in metabolic processes and almost 21% are related to reproduction, while several represent a variety of other cellular functions (Table 2).

To confirm the results obtained by mass spectrometry analysis, some of the most affected proteins were analyzed by Western blotting (Fig. 3). We were able to assess the amount of these proteins in the different fractions of male germ cells obtained by the STA-PUT method: the pachytene spermatocytes, the round spermatids, and the elongated spermatids (Fig. 3A). By quantifying the intensities of the bands in the elongated spermatids fraction, we confirmed that EIF4GI protein level was increased 3.5-fold in *Paip2a/Paip2b*-DKO mice when compared to WT (Fig. 3A and 3B). Interestingly, EIF4GI was increased 2.4-fold in round spermatids, as well (see Fig. 3A: 1.0 ± 0.12 in WT [$n = 3$], and 2.4 ± 0.3 in *Paip2a/Paip2b*-DKO mice [$n = 3$], $P < 0.05$). The increased levels of EIF4GI in DKO spermatids could be due to increased protein synthesis or decreased degradation. We also confirmed that AKAP4 was decreased to 20% and HK1-s was decreased to 25% in *Paip2a/Paip2b*-DKO elongated spermatids when compared to WT, suggesting the impaired translational control of these proteins in the absence of PAIP2A and PAIP2B during late spermiogenesis.

Effect of the Lack of PAIP2A and PAIP2B on Transcription in Spermiogenesis

In order to determine whether the results obtained using proteomic analysis were due to an impaired transcription regulation in the absence of PAIP2A and PAIP2B, we quantified the mRNA levels in elongated spermatids by real-time PCR (Fig. 4). We selected the three proteins for which changes had been confirmed by Western blot analysis. The relative mRNA level of the up-regulated protein, EIF4GI, in *Paip2a/Paip2b*-DKO mice was similar to that in WT mice (1.04-fold; Fig. 4A). The mRNA levels of the down-regulated protein, AKAP4, were unchanged in *Paip2a/Paip2b*-DKO

TABLE 1. Proteins that are significantly affected with at least 1.5-fold change in *Paip2a/Paip2b*-DKO as compared to WT elongated spermatids.*

Category	Accession no.	Protein name	Gene name	Unweighted spectrum counts (no.)†						Fold change
				WT1	WT2	WT3	DKO1	DKO2	DKO3	
Up-regulated	Q9D9D3	MCG9298	*Tbc1d21*	ND	ND	2	7	6	5	–
	Q3U3T8	WD repeat-containing protein 62	*Wdr62*	ND	ND	ND	7	7	12	–
	Q9CQX0	Ubiquitin thioesterase OTUB2	*Otub2*	2	3	3	9	9	11	3.625
	Q32MW4	Allantoicase	*Allc*	2	3	ND	7	5	5	3.400
	Q6NZJ6	Eukaryotic translation initiation factor 4 gamma 1	*Eif4g1*	4	8	8	16	20	25	3.050
	Q32MG2	Spermatid-associated protein	*Spert*	14	17	18	45	31	34	2.250
	Q9EP71	Ankycorbin	*Rai14*	4	3	3	9	8	5	2.200
	Q80X68	Citrate synthase	*Csl*	4	4	6	10	9	9	2.000
	O70252	Heme oxygenase 2	*Hmox2*	9	10	9	21	19	15	1.960
	Q8C605	Putative uncharacterized protein	*Pfkp*	2	4	6	8	8	7	1.910
	B2CY77	Laminin receptor	*Rpsa*	4	4	3	8	6	7	1.900
	Q9ESG2	Ropporin-1	*Ropn1*	5	6	5	10	12	8	1.875
	Q9DB77	Cytochrome b-c1 complex subunit 2, mitochondrial	*Uqcrc2*	4	5	6	8	10	9	1.800
	P58252	Elongation factor 2	*Eef2*	17	17	15	24	31	31	1.750
	Q9JMC3	DnaJ homolog subfamily A member 4	*Dnaja4*	8	7	7	13	11	14	1.720
	Q5SSW2	Proteasome activator complex subunit 4	*Psme4*	7	6	8	10	11	12	1.570
	P24369	Peptidyl-prolyl cis-trans isomerase B	*Ppib*	3	6	5	7	7	8	1.570
	A3R455	Cytochrome c oxidase subunit 2	*Cox2*	4	5	5	8	6	7	1.500
	P35487	Pyruvate dehydrogenase E1 component subunit alpha, testis-specific form, mitochondrial	*Pdha2*	8	7	11	13	14	12	1.500
Down-regulated	B2KF25	T-complex protein 11	*Tcp11*	10	12	12	7	6	8	1.620
	Q9DA79	Dipeptidase 3	*Dpep3*	14	9	15	7	7	8	1.730
	P15626	Glutathione S-transferase Mu 2	*Gstm2*	14	13	19	7	6	5	2.560
	Q8C5W0	Calmin	*Clmn*	16	16	16	ND	11	4	3.200
	A1EGX6	Fibrous sheath CABYR-binding protein	*Fscb*	8	7	8	2	ND	4	3.830
	Q3TJE3	Putative uncharacterized protein	*Hk1*	14	22	12	3	6	3	4.040
	Q9WV27	Sodium/potassium-transporting ATPase subunit alpha-4	*Atp1a4*	9	6	7	ND	3	2	4.400
	A1L3T6	A kinase (PRKA) anchor protein 4	*Akap4*	25	46	36	ND	ND	3	–
	P99024	Tubulin beta-5 chain	*Tubb5*	ND	42	41	ND	ND	ND	–
	P10649	Glutathione S-transferase Mu 1	*Gstm1*	12	13	20	ND	9	ND	–

* Proteins are shown from the highest to the lowest fold change for each category.
† ND, not detected.

mice as compared to WT mice (Fig. 4B). There are three isoforms of hexokinase 1 (*Hk1*) mRNA: the general *Hk1* and two spermatogenic cell-specific *mHk1-s* (*mHk1-sa* and *mHk1-sb*) containing a spermatogenic cell-specific sequence region (SSR). The peptide sequences obtained by proteomics assay were consensus sequences of both *Hk1* and testis-specific *Hk1-s* (Supplemental Fig. S3). Primers were designed to detect both the ubiquitous and the testis-specific forms of HK1. No amplification could be obtained using the ubiquitous *Hk1*. The mRNA corresponding to the testis-specific HK1-s was amplified from elongated spermatids, and we did not observe any change in the amount of this mRNA in *Paip2a*/*Paip2b*-DKO mice as compared to WT mice (Fig. 4C). Overall, these results suggest that the changes observed by proteomics were

TABLE 2. Biological function, number, and names of proteins significantly up- or down-regulated in the absence of PAIP2A and PAIP2B.

Biological function	Proteins (no.)	Gene name	
		Up-regulated	Down-regulated
Metabolism	8	*Allc, Csl, Hmox2, Pdha2, Pfkp*	*Gstm1, Gstm2, Hk1*
Reproduction	6	*Psme4, Spert*	*AKap4, Atp1a4, Fscb, Tcp11*
Protein catabolic process	4	*Otub2, Ppib, Uqcrc2*	*Ddep3*
Cytoskeleton	3	*Rai14*	*Clmn, Tubb5*
Translation	3	*Eef2, Eif4g1, Rpsa*	
Signal transduction	2	*Ropn1, Tbc1d21*	
Response to stress	1	*Dnaja4*	
Respiratory electron transport chain	1	*Cox2*	
Unknown	1	*Wrd62*	

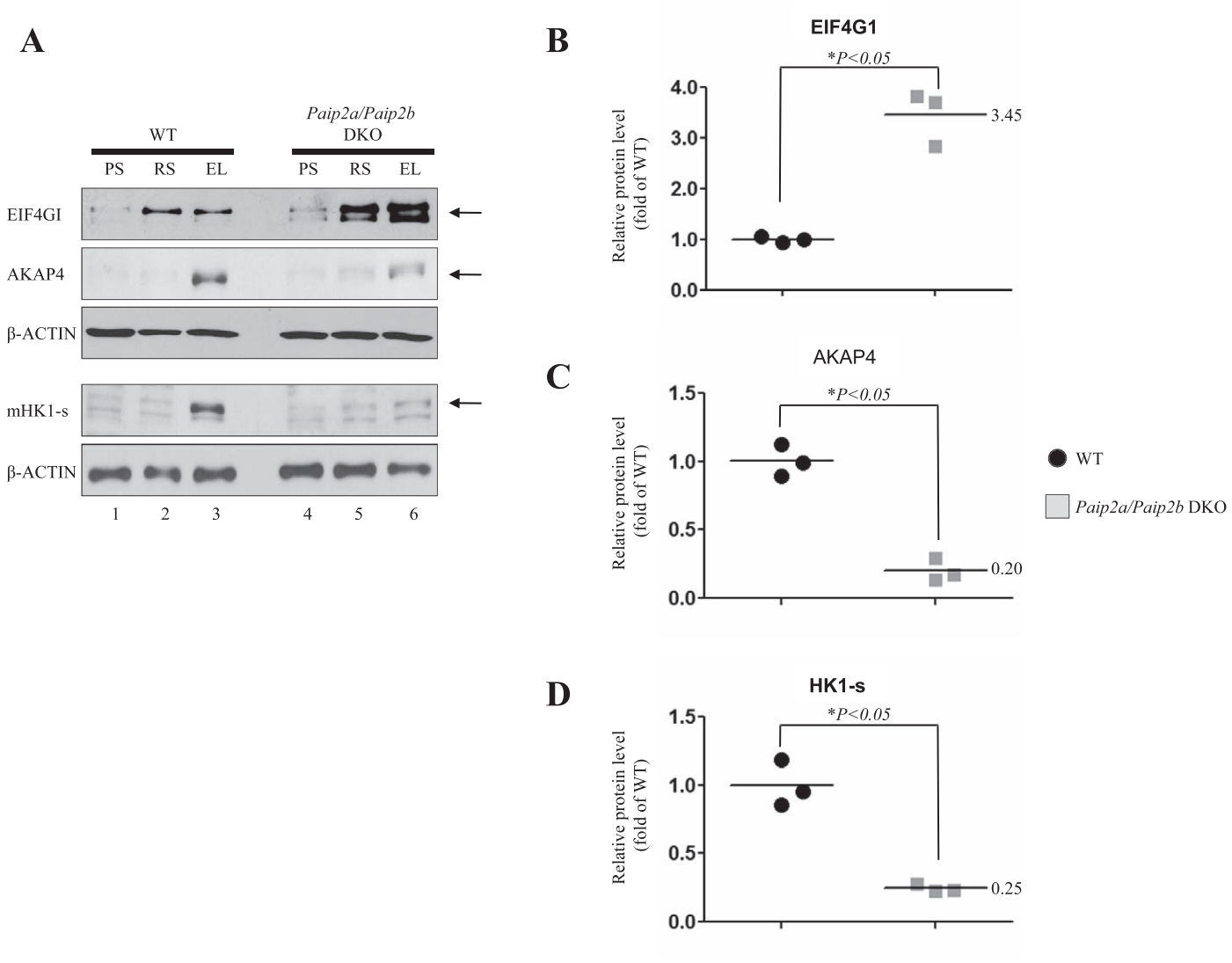

FIG. 3. **A**) Representative Western blot of three experiments for the EIF4G1, AKAP4, and HK1 proteins in the pachyteme spermatocytes (PS), round spermatids (RS), and elongated spermatids (EL) of WT and *Paip2a/Paip2b*-DKO mice. Quantitative analysis of the bands in the EL for EIF4GI (**B**), AKAP4 (**C**), and HK1-s (**D**). The intensities of the bands were measured using ImageJ (National Institutes of Health). The value of each band was normalized by that of β-actin. The band intensity in WT mice was set at one. $^*P < 0.05$ using an unpaired *t*-test (n = 3). Black circles indicate WT mice; gray squares indicate *Paip2a/Paip2b*-DKO mice.

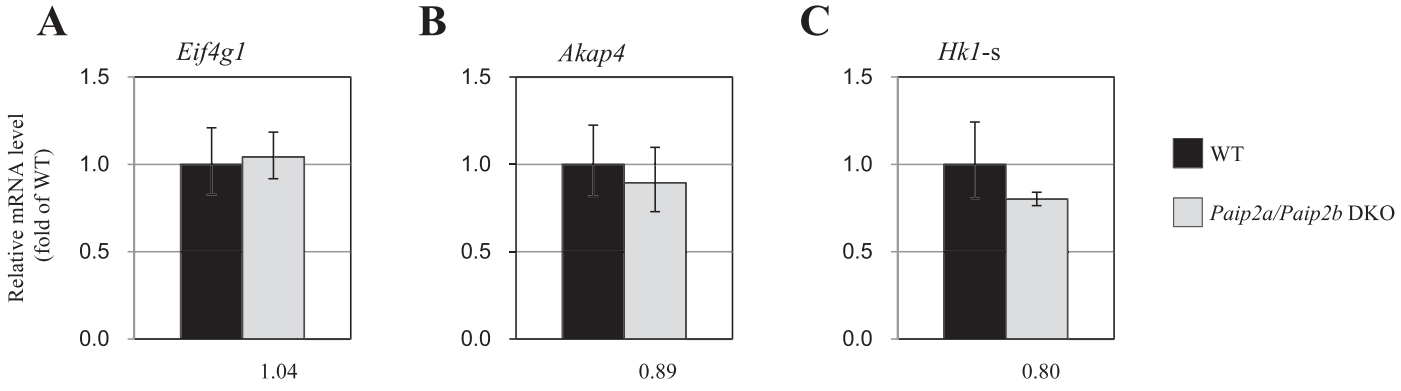

FIG. 4. Relative mRNA levels of *Eif4g1* (**A**), *Akap4* (**B**), and *Hk1*-s (**C**) in the elongated spermatids of WT mice (black bars) and *Paip2a/Paip2b*-DKO mice (gray bars). The *Actb* mRNA level in each sample was determined and used to normalize the differences of total RNA amount. Values indicate the relative mRNA levels in *Paip2a/Paip2b*-DKO mice as compared with those in WT mice, which were set as one. Statistical analysis was performed using an unpaired *t*-test (n = 3). No significant differences were observed.

TABLE 3. Tissue distribution of the down-regulated proteins in the absence of PAIP2A and PAIP2B, according to the literature.

Protein name	Protein localization	References
DPEP3	Testis specific	[40]
ATP1A4	Spermatids/spermatozoa specific Cauda sperm: Midpiece of the flagellum	[41, 42]
AKAP4	Spermatids/spermatozoa specific Fibrous sheath of the flagellum	[33, 43]
TCP11	Post meiotic male germ cell specific Cauda sperm: Acrosome and tail	[44, 45]
FSCB	Post meiotic male germ cells specific (steps 11 to 16 of spermiogenesis) Cauda sperm: fibrous sheath of the flagellum	[34]
CLMN (calmin)	Testis, brain, liver, kidney and large intestine Testis: Late spermatids	[46, 47]
HK1	Ubiquitous Testis: somatic and spermatogenic cell-specific transcripts variants Cauda sperm: fibrous sheath of the flagellum	[21]
GSTM1	Ubiquitous Testis: Sertoli cells, Leydig cells and germ cells	[27, 28, 48]
GSTM2	Ubiquitous Testis: Sertoli cells, Leydig cells and germ cells	[27, 28, 48]
TUBB5	Ubiquitous	[49]

most likely due to regulation at the protein level, such as translation and protein stability, rather than changes in transcripts.

Selective Translation Control by PAIP2A

Since PAIP2A is a key player of translation initiation during spermiogenesis [12], we speculated that proteins whose mRNAs are under translational control by PAIP2A would be down-regulated when compared to WT. For this reason, we further investigated the 10 down-regulated proteins in *Paip2a*/*Paip2b*-DKO mice and compared them with those of WT mice. Interestingly, four of these (i.e., AKAP4, ATP1A4, FSCB, and TCP11) are directly related to reproductive function according to the GO term database (http://www.geneontology.org/; Table 2). This suggests that PAIP2A is involved in the expression of specific proteins for male germ cell differentiation in late spermiogenesis. Moreover, all of these proteins are expressed in male germ cells (Table 3), and 50% of them (i.e., ATP1A4, AKAP4, TCP11, FSCB, and CLMN [CALMIN]) have been suggested to be under translational control, as they are spermatid specific (Table 3). These results strongly indicate that PAIP2A is a major factor controlling translation of mRNAs encoding these proteins.

DISCUSSION

In this study, we have characterized the proteins in the elongated spermatids from Stages 8 to 16 of spermiogenesis using a 1D gel coupled to MS/MS analysis. We identified 209 proteins that are consistently expressed with a level of expression higher than five unweighted spectrum counts. There is growing interest in the characterization of the proteome of male germ cells [23]. A recent study identified 2116 proteins from ICR mouse haploid germ cells using a similar strategy [24]. The discrepancy between this number and that obtained in our present study can be explained, at least in part, by the differences in cell sorting processes; in the present study, we excluded the early stage of spermiogenesis (i.e., the round spermatids) and characterized the proteins expressing in late spermiogenesis.

We have further demonstrated that the expression of several proteins was affected by the absence of PAIP2A and PAIP2B. Considering that PAIP2A is much more abundant than PAIP2B in the testis [12], and that only the *Paip2a*- but not the *Paip2b*-KO male mice are infertile [12], it is very likely that PAIP2A is responsible for translational control in late spermiogenesis.

PAIP2A has been characterized as a general translational regulator [14]. Surprisingly, only some proteins were up- or down-regulated in *Paip2a*/*Paip2b*-DKO elongated spermatids, suggesting that PAIP2 might regulate translation of specific mRNAs. Interestingly, other studies have shown that knockouts of genes encoding factors that are expected to affect general translation appear to affect translation of specific mRNAs in male germ cells [15, 25]. We have previously demonstrated that PAIP2A controls, in part, translation of the transition proteins and protamine 1 during late spermiogenesis in *Paip2a*/*Paip2b*-DKO mice [12]. Therefore, in this study, we hypothesized that the down-regulated proteins in the *Paip2a*/*Paip2b*-DKO mice might be controlled by PAIP2A. Surprisingly, we only observed 10 significantly down-regulated proteins, including two that were totally missing in *Paip2a*/*Paip2b*-DKO elongated spermatids: TUBB5 and GSTM1. To our knowledge, translational control of TUBB5 and GSTM1 during spermiogenesis had not been described previously. Imunohistochemical studies showed that GSTs are mainly expressed in testicular somatic cells [26–28], especially in the Sertoli cells. However, studies assessing GST activity in purified testicular cell populations have shown activity in all cell types, including the germ cells [29, 30]. Various isoforms of GSTs are present on sperm plasma membranes and in the cytosolic compartment [31]. Their main role is considered to be to help protect sperm from chemical insult, but some isoforms have been localized also to the fibrous sheath [32], anchoring an enzymatic complex to a specific cellular compartment.

Our results suggest that the 10 significantly down-regulated proteins might be targets of PAIP2A in translation control. Interestingly, five of these proteins are exclusively expressed in spermatids. Moreover, protein expression of AKAP4, ATP1A4, and FSCB is regulated under translational control in late spermiogenesis (see Table 3 for references); these observations fit well with our proposed model, in which PAIP2A regulates translation of the proteins needed for late spermiogenesis. It is interesting to note that seven of the 10 down-regulated proteins are expressed in the flagellum of spermatozoa (Table 3). Furthermore, it has been shown that AKAP4, HK1, and FSCB interact and are involved in the late steps of fibrous sheath

development [33, 34]. These results suggest that PAIP2A is specifically involved in regulating translation of mRNAs encoding proteins necessary for biogenesis of the flagellum. This clearly correlates with the phenotype observed in the *Paip2a*/*Paip2b*-DKO and the *Paip2a*-KO, where we observed an impairment of flagellum formation associated with the absence of the mitochondrial sheath in the middle piece [12]. Interestingly, *Akap4*-KO mice [20] have abnormalities in the fibrous sheath and the outer dense fibers similar to those found in the *Paip2a*/*Paip2b*-DKO testis [12].

The mechanism by which PAIP2A selectively regulates the expression of specific RNAs is unknown. Transcriptional and post-transcriptional mechanisms during spermatogenesis are unique and have been reviewed [1, 35, 36], but little is known about RNA stabilization and translation during spermiogenesis. The male infertility found in *Paip2a*/*Paip2b*-DKO and *Paip2a*-KO mice suggests an important role for PAIP2A in spermatogenesis [12]. We previously demonstrated that efficient translation occurs at an optimal concentration of PABP, which is regulated by PAIP2A [12]. Indeed, excess amounts of PABP compete with EIF4G1, resulting in translational inhibition [12]. We confirmed in the present study that PABP expression was increased in the elongated spermatids of *Paip2a*/*Paip2b*-DKO when compared to WT; nevertheless, such a mechanism alone would not be sufficient to explain the regulation of specific mRNAs in our model. It is possible that there are regulatory *cis*-elements in these RNAs, such as a specific sequence in the 3′ untranslated region (UTR). For example, Zhong et al. [37] have characterized a highly conserved sequence in the 3′ UTR region of the protamine 1 mRNA that is necessary for translation repression. It is possible that these regulatory *cis*-elements in specific mRNAs might modulate the affinity of PABP to poly (A) tail together with PAIP2A. Further studies comparing the sequence of the RNAs of up- and down-regulated proteins in the *Paip2a*/*Paip2b*-DKO are needed to investigate the possibility of such regulatory sequences.

In this study, we have also shown that 19 proteins were significantly up-regulated in the *Paip2a*/*Paip2b*-DKO elongated spermatids. These proteins are involved in various biological functions, but mostly in metabolism. It is important to consider the aberrant spermatid differentiation in the *Paip2a*/*Paip2b*-DKO and *Paip2a*-KO mice [12] that is likely to involve variation in cellular components, indirectly resulting in changes of protein levels. One possible explanation for up-regulated proteins is that the translation of mRNAs encoding proteins involved in degradation processes is inhibited. To our knowledge, no obvious candidate for involvement in protein degradation processes can be found in the significantly up-regulated proteins in the *Paip2a*/*Paip2b*-DKO. It has been suggested that the ubiquitin-proteasome pathway plays a major role during spermatogenesis [38, 39], and, interestingly, members of the proteasome complex, such as the proteasome activator complex subunit 4, have been detected by mass spectrometry. Further study of proteins involved in the degradation pathway found by our proteomics analysis using elongated spermatids should be informative.

In summary, these studies have revealed a number of proteins that could be targets of PAIP2A-dependent translational control. Moreover, we identified the up-regulated proteins present in elongated spermatids, and several uncharacterized proteins were also revealed. The function of some of these proteins in late spermiogenesis is known, while that of many others remains to be identified.

ACKNOWLEDGMENT

We would like to thank Dr. E.M. Eddy for the gift of the AKAP4 and HK1 antibodies. We also wish to thank Drs. Eddy Rijntjes and Marcos Di Falco for their help in data analysis under Scaffold 2.0 and discussions of statistical analysis.

REFERENCES

1. Bettegowda A, Wilkinson MF. Transcription and post-transcriptional regulation of spermatogenesis. Philos Trans R Soc Lond B Biol Sci 2010; 365:1637–1651.
2. Gu W, Kwon Y, Oko R, Hermo L, Hecht NB. Poly (A) binding protein is bound to both stored and polysomal mRNAs in the mammalian testis. Mol Reprod Dev 1995; 40:273–285.
3. Kimura M, Ishida K, Kashiwabara S, Baba T. Characterization of two cytoplasmic poly(A)-binding proteins, PABPC1 and PABPC2, in mouse spermatogenic cells. Biol Reprod 2009; 80:545–554.
4. Kleene KC, Wang MY, Cutler M, Hall C, Shih D. Developmental expression of poly(A) binding protein mRNAs during spermatogenesis in the mouse. Mol Reprod Dev 1994; 39:355–364.
5. Xu M, Hecht NB. Polypyrimidine tract binding protein 2 stabilizes phosphoglycerate kinase 2 mRNA in murine male germ cells by binding to its 3′UTR. Biol Reprod 2007; 76:1025–1033.
6. Xu M, Hecht NB. MSY2 and polypyrimidine tract binding protein 2 stabilize mRNAs in the mammalian testis. Int J Androl 2008; 31:457–461.
7. Yang J, Medvedev S, Yu J, Tang LC, Agno JE, Matzuk MM, Schultz RM, Hecht NB. Absence of the DNA-/RNA-binding protein MSY2 results in male and female infertility. Proc Natl Acad Sci U S A 2005; 102:5755–5760.
8. Yang J, Medvedev S, Reddi PP, Schultz RM, Hecht NB. The DNA/RNA-binding protein MSY2 marks specific transcripts for cytoplasmic storage in mouse male germ cells. Proc Natl Acad Sci U S A 2005; 102:1513–1518.
9. Yang J, Morales CR, Medvedev S, Schultz RM, Hecht NB. In the absence of the mouse DNA/RNA-binding protein MSY2, messenger RNA instability leads to spermatogenic arrest. Biol Reprod 2007; 76:48–54.
10. Paronetto MP, Messina V, Bianchi E, Barchi M, Vogel G, Moretti C, Palombi F, Stefanini M, Geremia R, Richard S, Sette C. Sam68 regulates translation of target mRNAs in male germ cells, necessary for mouse spermatogenesis. J Cell Biol 2009; 185:235–249.
11. Tsai-Morris CH, Sheng Y, Lee E, Lei KJ, Dufau ML. Gonadotropin-regulated testicular RNA helicase (GRTH/Ddx25) is essential for spermatid development and completion of spermatogenesis. Proc Natl Acad Sci U S A 2004; 101:6373–6378.
12. Yanagiya A, Delbes G, Svitkin YV, Robaire B, Sonenberg N. The poly(A)-binding protein partner Paip2a controls translation during late spermiogenesis in mice. J Clin Invest 2010; 120:3389–3400.
13. Karim MM, Svitkin YV, Kahvejian A, De CG, Costa-Mattioli M, Sonenberg N. A mechanism of translational repression by competition of Paip2 with eIF4G for poly(A) binding protein (PABP) binding. Proc Natl Acad Sci U S A 2006; 103:9494–9499.
14. Khaleghpour K, Svitkin YV, Craig AW, DeMaria CT, Deo RC, Burley SK, Sonenberg N. Translational repression by a novel partner of human poly(A) binding protein, Paip2. Mol Cell 2001; 7:205–216.
15. Kashiwabara S, Noguchi J, Zhuang T, Ohmura K, Honda A, Sugiura S, Miyamoto K, Takahashi S, Inoue K, Ogura A, Baba T. Regulation of spermatogenesis by testis-specific, cytoplasmic poly(A) polymerase TPAP. Science 2002; 298:1999–2002.
16. Kleene KC. Poly(A) shortening accompanies the activation of translation of five mRNAs during spermiogenesis in the mouse. Development 1989; 106:367–373.
17. Bellve AR, Millette CF, Bhatnagar YM, O'Brien DA. Dissociation of the mouse testis and characterization of isolated spermatogenic cells. J Histochem Cytochem 1977; 25:480–494.
18. Meistrich ML, Bruce WR, Clermont Y. Cellular composition of fractions of mouse testis cells following velocity sedimentation separation. Exp Cell Res 1973; 79:213–227.
19. Zhu W, Smith JW, Huang CM. Mass spectrometry-based label-free quantitative proteomics. J Biomed Biotechnol 2010; 2010:840518.
20. Miki K, Willis WD, Brown PR, Goulding EH, Fulcher KD, Eddy EM. Targeted disruption of the Akap4 gene causes defects in sperm flagellum and motility. Dev Biol 2002; 248:331–342.
21. Mori C, Nakamura N, Welch JE, Gotoh H, Goulding EH, Fujioka M, Eddy EM. Mouse spermatogenic cell-specific type 1 hexokinase (mHk1-s) transcripts are expressed by alternative splicing from the mHk1 gene and

the HK1-S protein is localized mainly in the sperm tail. Mol Reprod Dev 1998; 49:374–385.
22. Barcellona WJ, Meistrich ML. Ultrastructural integrity of mouse testicular cells separated by velocity sedimentation. J Reprod Fertil 1977; 50:61–68.
23. Huang XY, Sha JH. Proteomics of spermatogenesis: from protein lists to understanding the regulation of male fertility and infertility. Asian J Androl 2011; 13:18–23.
24. Guo X, Shen J, Xia Z, Zhang R, Zhang P, Zhao C, Xing J, Chen L, Chen W, Lin M, Huo R, Su B, et al. Proteomic analysis of proteins involved in spermiogenesis in mouse. J Proteome Res 2010; 9:1246–1256.
25. Sun F, Palmer K, Handel MA. Mutation of Eif4g3, encoding a eukaryotic translation initiation factor, causes male infertility and meiotic arrest of mouse spermatocytes. Development 2010; 137:1699–1707.
26. Papp S, Robaire B, Hermo L. Developmental expression of the glutathione S-transferase Yo subunit in the rat testis and epididymis using light microscope immunocytochemistry. Anat Rec 1994; 240:345–357.
27. Veri JP, Hermo L, Robaire B. Immunocytochemical localization of the Yf subunit of glutathione S-transferase P shows regional variation in the staining of epithelial cells of the testis, efferent ducts, and epididymis of the male rat. J Androl 1993; 14:23–44.
28. Veri JP, Hermo L, Robaire B. Immunocytochemical localization of glutathione S-transferase Yo subunit in the rat testis and epididymis. J Androl 1994; 15:415–434.
29. Bauche F, Fouchard MH, Jegou B. Antioxidant system in rat testicular cells. FEBS Lett 1994; 349:392–396.
30. Yoganathan T, Eskild W, Hansson V. Investigation of detoxification capacity of rat testicular germ cells and Sertoli cells. Free Radic Biol Med 1989; 7:355–359.
31. Rao AV, Shaha C. Multiple glutathione S-transferase isoforms are present on male germ cell plasma membrane. FEBS Lett 2001; 507:174–180.
32. Nakamura N, Mori C, Eddy EM. Molecular complex of three testis-specific isozymes associated with the mouse sperm fibrous sheath: hexokinase 1, phosphofructokinase M, and glutathione S-transferase mu class 5. Biol Reprod 2010; 82:504–515.
33. Brown PR, Miki K, Harper DB, Eddy EM. A-kinase anchoring protein 4 binding proteins in the fibrous sheath of the sperm flagellum. Biol Reprod 2003; 68:2241–2248.
34. Li YF, He W, Jha KN, Klotz K, Kim YH, Mandal A, Pulido S, Digilio L, Flickinger CJ, Herr JCFSCB. a novel protein kinase A-phosphorylated calcium-binding protein, is a CABYR-binding partner involved in late steps of fibrous sheath biogenesis. J Biol Chem 2007; 282:34104–34119.
35. Tanaka H, Baba T. Gene expression in spermiogenesis. Cell Mol Life Sci 2005; 62:344–354.
36. Kleene KC. Patterns, mechanisms, and functions of translation regulation in mammalian spermatogenic cells. Cytogenet Genome Res 2003; 103:217–224.
37. Zhong J, Peters AH, Kafer K, Braun RE. A highly conserved sequence essential for translational repression of the protamine 1 messenger RNA in murine spermatids. Biol Reprod 2001; 64:1784–1789.
38. Mochida K, Tres LL, Kierszenbaum AL. Structural features of the 26S proteasome complex isolated from rat testis and sperm tail. Mol Reprod Dev 2000; 57:176–184.
39. Sutovsky P. Ubiquitin-dependent proteolysis in mammalian spermatogenesis, fertilization, and sperm quality control: killing three birds with one stone. Microsc Res Tech 2003; 61:88–102.
40. Habib GM, Shi ZZ, Cuevas AA, Lieberman MW. Identification of two additional members of the membrane-bound dipeptidase family. FASEB J 2003; 17:1313–1315.
41. Shamraj OI, Lingrel JB. A putative fourth Na+, K(+)-ATPase alpha-subunit gene is expressed in testis. Proc Natl Acad Sci U S A 1994; 91:12952–12956.
42. Wagoner K, Sanchez G, Nguyen AN, Enders GC, Blanco G. Different expression and activity of the alpha1 and alpha4 isoforms of the Na, K-ATPase during rat male germ cell ontogeny. Reproduction 2005; 130:627–641.
43. Carrera A, Gerton GL, Moss SB. The major fibrous sheath polypeptide of mouse sperm: structural and functional similarities to the A-kinase anchoring proteins. Dev Biol 1994; 165:272–284.
44. Hosseini R, Ruddy S, Bains S, Hynes G, Marsh P, Pizzey J, Dudley K. The mouse t-complex gene, Tcp-11, is under translational control. Mech Dev 1994; 47:73–80.
45. Fraser LR, Hosseini R, Hanyalogou A, Talmor A, Dudley RK. TCP-11, the product of a mouse t-complex gene, plays a role in stimulation of capacitation and inhibition of the spontaneous acrosome reaction. Mol Reprod Dev 1997; 48:375–382.
46. Ishisaki Z, Takaishi M, Furuta I, Huh N. Calmin, a protein with calponin homology and transmembrane domains expressed in maturing spermatogenic cells. Genomics 2001; 74:172–179.
47. Marzinke MA, Henderson EM, Yang KS, See AW, Knutson DC, Clagett-Dame M. Calmin expression in embryos and the adult brain, and its regulation by all-trans retinoic acid. Dev Dyn 2010; 239:610–619.
48. Sheehan D, Meade G, Foley VM, Dowd CA. Structure, function and evolution of glutathione transferases: implications for classification of non-mammalian members of an ancient enzyme superfamily. Biochem J 2001; 360:1–16.
49. Lewis SA, Lee MG, Cowan NJ. Five mouse tubulin isotypes and their regulated expression during development. J Cell Biol 1985; 101:852–861.